NISH-M 65-0791

DEC 10 1965

A Reprint from

PROCEEDINGS
OF
THE EIGHTH JAPAN CONGRESS
ON
TESTING MATERIALS

Published by

THE SOCIETY OF MATERIALS SCIENCE, JAPAN

KYOTO, JAPAN 1965

EFFECT OF HYDROSTATIC PRESSURE ON MECHANICAL BEHAVIOUR OF MATERIALS (THE SECOND REPORT)

By Masao NISHIHARA*, Kichinosuke TANAKA**
and Hiroyoshi HAMADA***

1. Introduction

In the previous work[1] on the effect of hydrostatic pressure on mechanical behaviour of materials, the load applied to a test specimen was obtained indirectly by subtracting the frictional force between the piston and the packings from the load indicated by dynamometer of testing machine. The frictional force, however, is greatly affected by hydrostatic pressure. Especially at high hydrostatic pressure and at the beginning of displacement of the piston, this frictional force is quite unstable, so it was very difficult to know the accurate value of the load applied to the test specimen.

In an effort to measure the load correctly a load cell which can be used under high hydrostatic pressure, has been successfully developed. In order to observe a specimen during the testing, optical windows were made in the wall of the high pressure cylinder. The followings are some results obtained by using the load cell and the optical windows mentioned above.

2. Equipment and Procedure

The improved apparatus is schematically shown in Fig. 1 where L is the load cell, S a test specimen, W the optical window and P the piston. When a load is applied by a universal testing machine, the upper piston pushes dwon the bottom of the test specimen in a high pressure cylinder. The load cell mounted between the piston and the push-bar will indicate the tensile load applied to the test specimen. The load cell is made of a steel core and strain gauges bonded to the core. The load cell may deform under hydrostatic pressure and there will be some strain-output as the result. But the strain-output is linearly proportional to the hydrostatic pressure applied.

With axial load the strain-output of load cell has another linear relationship which is the same as at atmospheric pressure. Fig. 2 shows the relation between the axial load and the strain-output of load cell. So we will be able to determine the axial load applied to test specimen during the test under hydrostatic pressure. As the strain of a test specimen is relatively large, it

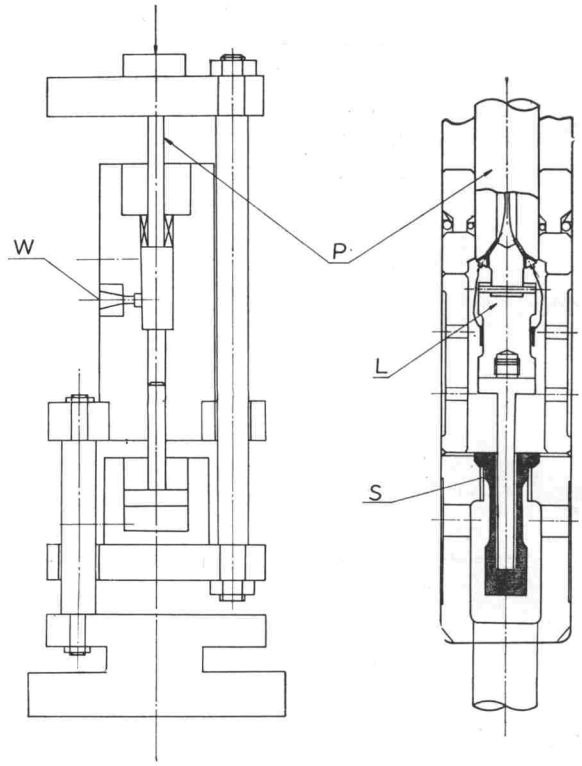


Fig. 1. Testing Apparatus.

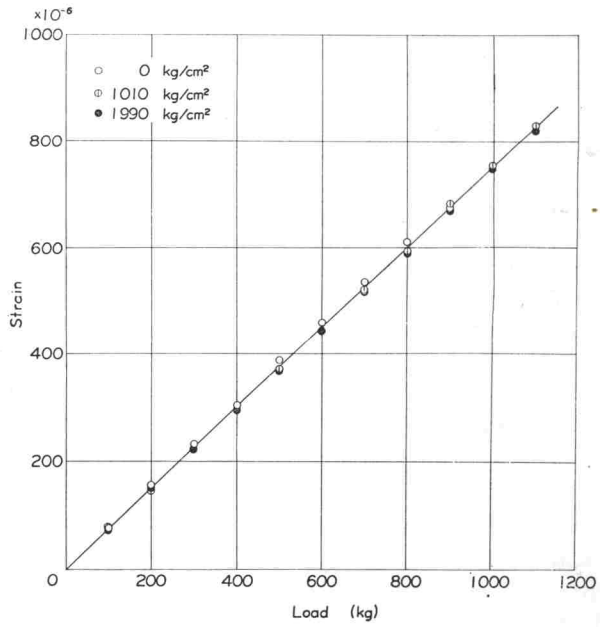


Fig. 2. Calibration Curve of Load Cell under Hydrostatic Pressure.

*, *** *Department of Mechanical Engineering, Doshisha University; Member of the Society of Materials Science, Japan*

** *Faculty of Engineering, Kyoto University; Member of the Society of Materials Science, Japan, of the Japan Society of Mechanical Engineers, of the Japan Society for Aeronautical and Space Sciences and of the Japan Institute of Metals*

is sufficient to measure the displacement of the piston by using a π-gauge, instead of measuring the elongation of the test specimen in the high pressure cylinder. The load-elongation diagrams were recorded automatically by an X-Y recorder connected to the load cell and the π-gauge and also to the differential transformer extensometer. The pressure-transmitting medium is silicone oil. In the previous experiment[1] white spindle oil was used, but the image of a test specimen through the optical window disappeared above the hydrostatic pressure of about 1,800 kg/cm^2.

3. Materials and Specimens

The materials tested are carbon steel, titanium, zirconium, aluminium, cast zinc and Mg-Al alloy. The chemical composition of these materials are given in Table 1. The specimens of carbon steel were annealed

Table 1. Chemical Composition of Materials Tested (%).

Carbon Steel	C 0.09	Mn 0.52	Si 0.17	P 0.009	S 0.026	Cu 0.11	Ni 0.04	Cr 0.03
Titanium	H_2 0.015	O_2 0.078	N_2 0.035	Si 0.017	Fe 0.050	C 0.01	Ti Balance	
Zirconium	H_2 0.0043	O_2 0.051	N_2 0.002	Si 0.005	Fe 0.083	C 0.008	Hf 0.04	Zr Balance
Aluminium	Si 0.06	Cu 0.0031	Fe 0.03	Al Balance				
Zinc	Pb 0.0008	Cd 0.098	Fe 0.001	Sn <0.0001	Zn Balance			
Mg-Al Alloy	Al 0.87	Be 0.008	Si 0.003	Fe 0.006	Cu 0.0003	Mg Balance		

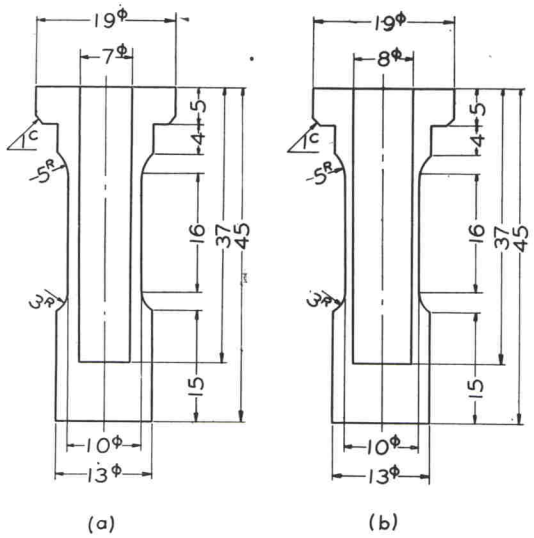


Fig. 3. Specimens (a), (b).

in vacuum for one hour at 900°C and those of aluminium for one hour at 400°C after machining, but other materials were tested without any heat treatment. The shape and the size of the test specimens are given in Fig. 3 (a), (b). (a) is for aluminium, zinc and Mg-Al alloy and (b) for carbon steel, titanium and zirconium.

4. Results and Discussions

An example of the automatically recorded load-elongation diagram is shown in Fig. 4 (carbon steel, hydrostatic pressure: 1,040 kg/cm^2). From these load-elongation diagrams at different pressure, we got the stress-stain curves. Fig. 5 shows the curves for carbon steels. In this figure, the ordinate shows the differential

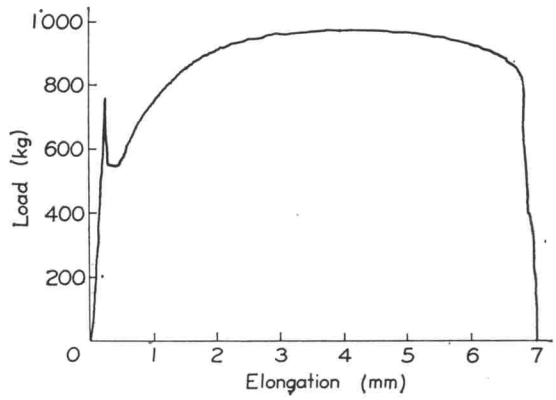


Fig. 4. Recorded Load-Elongation Diagram of Carbon Steel at the Pressure of 1,040 kg/cm^2.

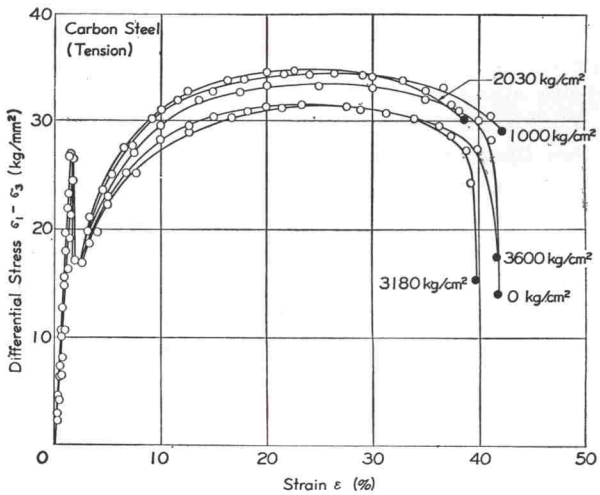


Fig. 5. Stress-Strain Curves of Carbon Steel.

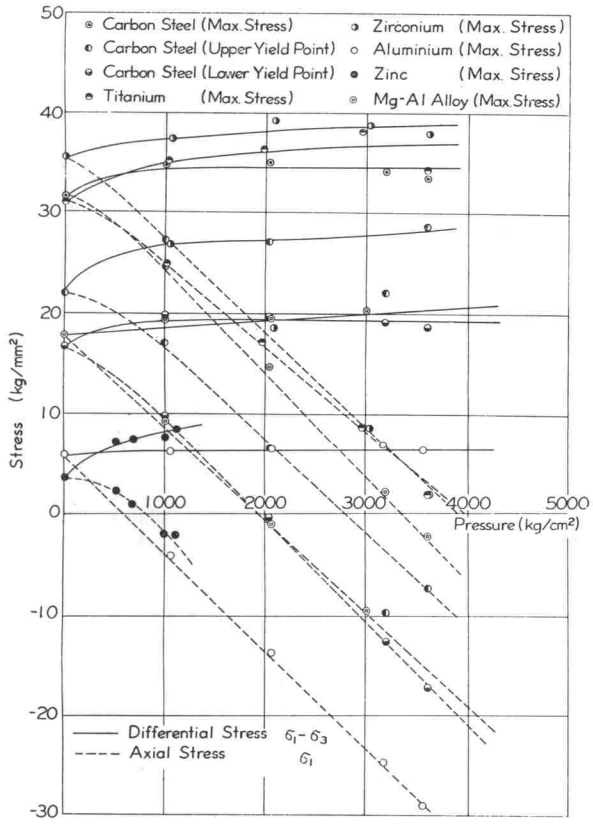


Fig. 6. Effect of Pressure on Upper and Lower Yield Point and Maximum Stress.

stress $\sigma_1-\sigma_3$ (kg/mm^2) and the abscissa the strain ε (%). The relationship between the hydrostatic pressure and the maximum differential stress (for carbon steel, the upper and lower yield point and the maximum differential stress respectively) is given in Fig. 6. In general the maximum differential stresses increase slightly with pressure.

From the experimental results, the longitudinal, the radial and the tangential strain are calculated. If we denote the initial gauge length by l_0, the gauge length after deformation l; the initial cross-sectional area A_0, the cross-sectional area at the neck after deformation A; the initial wall thickness t_0 and the thickness after deformation t; the initial mean radius r_0 and the mean radius after deformation r, the longitudinal-natural strain is expressed by ln (l/l_0), which is equal to ln (A_0/A) assuming the constancy of volume and taking the gauge length within the necked part. And also the radial-natural strain is given by ln (t/t_0) and the tangential-natural strain ln (r/r_0). The relation between the radial-natural strain and the pressure is given in Fig. 7. The radial-natural strain generally increases with the pressure, and for aluminium it increases remarkably. There exists a very remarkable increase for zinc at the hydrostatic pressure of about 1,000 kg/cm^2. Fig. 8 is a diagram showing the relation between the longitudinal-natural strain and the pressure. The longitudinal-natural strain also increases with the pressure and its tendency is similar

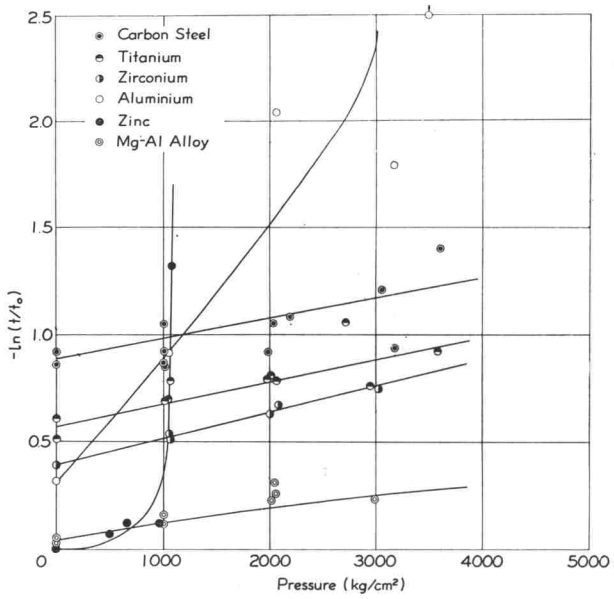


Fig. 7. Effect of Pressure on the Radial-Natural Strain at the Neck after Deformation.

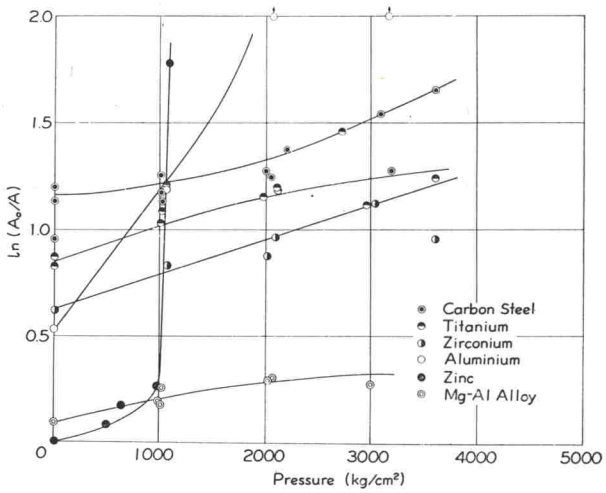


Fig. 8. Effect of Pressure on the Longitudinal-Natural Strain at the Neck after Deformation.

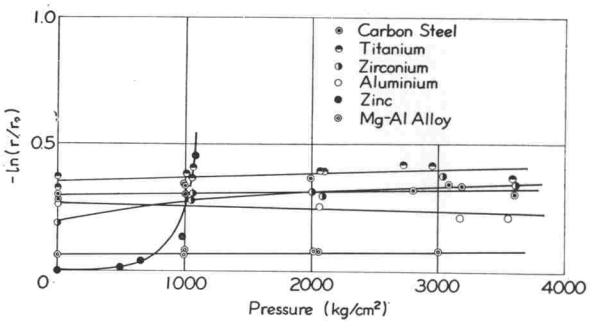


Fig. 9. Effect of Pressure on the Tangential-Natural Strain at the Neck after Deformation.

to Fig. 7, while the longitudinal-natual strain is larger than the radial-natural strain. The relation between the tangential-natural strain and the pressure is shown in Fig. 9 and the tangential-natural strain also increases

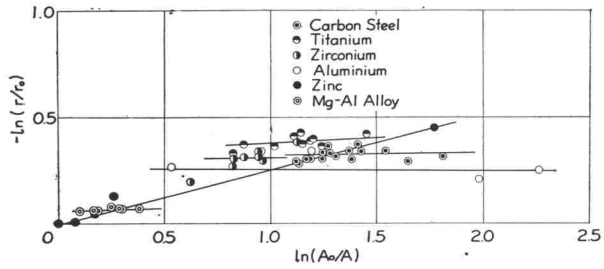


Fig. 10. The Tangential-Natural Strain against the Longitudinal-Natural Strain after Deformation.

with the pressure, but it decreases with the pressure for aluminium. The tangential-natural strain is about one third of the radial-, longitudinal-natural strains. For such exceptional behaviour of aluminium, we have not yet any reasonable explanation. In Fig. 10, the relation between the tangentinal-natural strain and the longitudinal-natural strain for various materials is given. Although different materials have different curves, the tangential-natural strain for the materials tested, except zinc, becomes nearly constant irrespective of the longitudinal-natural strain. In other words, as deformation proceeds to a certain extent, the tangential-natural strain becomes nearly constant. We have reported[1] that the specimens of titanium and zirconium were sucked in at its central part, even at atmospheric pressure. Judging from Fig. 10, it will be clearly understood that the more the tangential-natural strain increases, the more the central part of the specimen is sucked in. The relation between the radial-natural strain and the longitudinal-natural strain at fracture under various kinds of pressure is given in Fig. 11. This shows that as the hydrostatic pressure increases, the specimen elongates, and that the wall thickness of the test specimen becomes thin in proportion to the elongation of the test specimen.

The deformation of the test specimen was observed through the optical window during the testing. A test specimen can be considered as symmetric to its axis even after it deformed, so it is sufficient to observe the

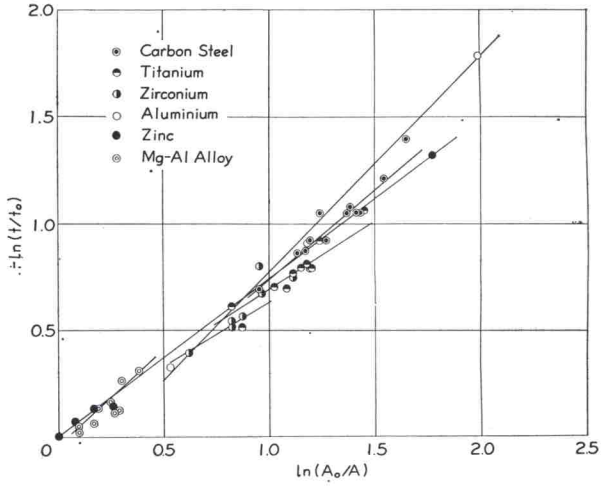


Fig. 11. The Radial-Natural Strain against the Longitudinal-Natural Strain at Fracture.

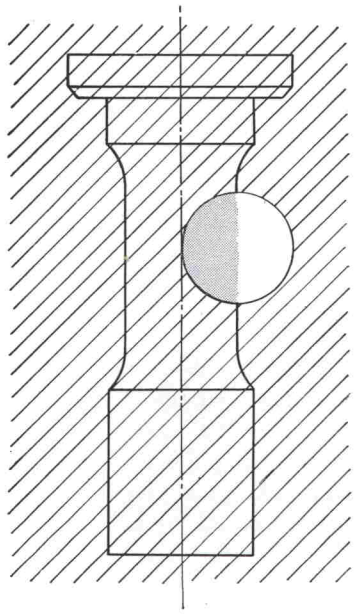
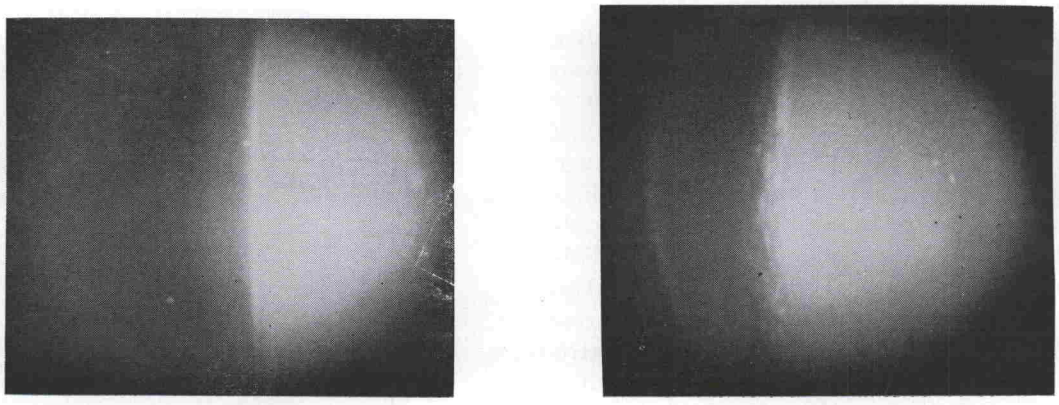


Fig. 12. Observation of Test Specimen through Optical Window.



(a)
$\sigma_1-\sigma_3=0$ kg/mm²
$\varepsilon=0\%$

(b)
$\sigma_1-\sigma_3=29.5$ kg/mm²
$\varepsilon=43.0\%$

Photo. 1. Titanium Specimen observed through Optical Window during a Test at the Pressure of 1,010 kg/cm².

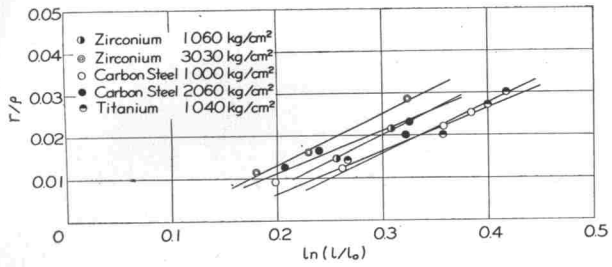


Fig. 13. The Ratio of the Outer Radius of the Test Specimen to the Radius of Longitudinal Curvature against the Longitudinal-Natural Strain.

half of the test specimen. Fig. 12 shows the part of a test specimen which can be observed through the optical window. The titanium specimen during test at the pressure of 1,010 kg/cm² is shown in Photo. 1. As shown in Fig. 13, the ratio of the outer radius of the test specimen to the radius of longitudinal curvature r/ρ, that is, the ratio of local contraction, increases linearly, with the longitudinal-natural strain $ln(l/l_0)$. During the test we can not observe the inside of a test specimen through the optical window, so we measure the elongation of the test specimen for determining the longitudinal-natural strain. Although the inclination of the curve is specific to a material, with the increase of hydrostatic pressure the curves move to the left of the diagram while its inclination remains constant for the same materials.

5. Conclusion

By using a load cell, we measured directly the load applied to a specimen under hydrostatic pressure. The experimental results thus obtained are similar to the results previously reported. But the dependence of the increase in the maximum differential stress on hydrostatic pressure is less conspicuous than the previous work.

The longitudinal-, the radial- and the tangential-natural strain after the testing are calculated from the experimental results and we obtained the relation between these strains and the pressure. In general these strains increase with the pressure. However, these strains for zinc increase suddenly at the pressure of about 1,000 kg/cm², and for aluminium the longitudinal and the radial-natural strain increase remarkably with the hydrostatic pressure. There is a linear relation between the longitudial-natural strain and the radial-natural strain. The tangential-natural strain is almost constant irrespective of the longitudinal-natural strain.

The deformation of a test specimen was observed through the optical windows during the test. The ratio of local contraction which was calculated from the deformation of the test specimen, seems to be a function of the longitudinal-natural strain and the hydrostatic pressure.

Acknowledgement

The improvement of the experimental installation was supported by grants from the Ministry of Education. The helpful suggestions by Mr. H. Ll. D. Pugh in National Engineering Laboratory and Dr. M. Yasunami in Kobe Steel Works, Ltd. are gratefully acknowledged.

Reference

1) M. Nishihara, K. Tanaka and T. Muramatsu : Proc. 7th Jap. Cong. Test. Mat., 154 (1964)